C fold in several ways. The seven β strands of E-CAD1 are all connected by interstrand hydrogen bonds to form an almost completely cylindrical β barrel. The Ig C domain, on the other hand, consists of two distinct β sheets to which additional strands are added to form other variants of the Ig fold (9). The greater twist of the β sheets required to form a cylindrical β barrel results in a more obtuse angle between the directions of the packed β strands in the CAD domain. Thus, the structures of the two domains are virtually nonsuperimposable. The metal binding pocket found in E-CAD1 is absent in the Ig C domain (9), whereas the conserved disulfide bond between βB and βF of the Ig C fold is not present in CAD domains. Membrane-proximal CAD5 domains contain four conserved cysteine residues (Fig. 1C) that may form a disulfide bond or bonds (15). In light of the structures of E-CAD1 and an Ig domain in CD2 containing a disulfide bond (9), the first cysteine residue of CAD5 (Fig. 1C) is able to form a disulfide bond with the second or third cysteine of CAD5, thus stabilizing the βA'-βG pairing.

Topological similarities between individual extracellular domains of cadherins and Ig CAMs identified here can be explained either by divergent or convergent evolution. An ancestral CAM domain may have diverged into Ca^{2+}-dependent and Ca^{2+}-independent forms while retaining modular features that are still shared by the cadherin and Ig superfamilies. Alternatively, the independent evolution of analogous extracellular domains by these two superfamilies would attest to the stability and particular suitability of this β-barrel fold for cell-cell adhesion.

REFERENCES AND NOTES

1. M. Takeichi, *Annu. Rev. Biochem.* **59**, 237 (1990); G. M. Edelman and K. L. Crossin, *ibid.* **60**, 155 (1991).
2. M. Takeichi, *Curr. Opin. Cell Biol.* **5**, 806 (1993).
3. A. Nose, K. Tsuji, M. Takeichi, *Cell* **61**, 147 (1990).
4. M. Ozawa *et al.*, *EMBO J.* **8**, 1711 (1989); A. Nagafuchi and M. Takeichi, *Cell Regul.* **1**, 37 (1989).
5. The purification, Ca^{2+}-binding properties, and monomeric state of the recombinant polypeptide comprising amino acids 1 to 144 plus two more NH_2-terminal amino acids of mouse E-cadherin have been described by K. I. Tong *et al.* [*FEBS Lett.* **352**, 318 (1994)]. ^{15}N-labeled, $^{13}C/^{15}N$-labeled, or unlabeled protein was dissolved to 0.5 to 2 mM in either 95% H_2O plus 5% ^2H_2O or 99.996% ^2H_2O containing 100 mM KCl, 10 mM perdeuterated dithiothreitol, 20 mM perdeuterated tris, and 50 μM NaN_3 and 10 mM $CaCl_2$ (except for the Ca^{2+}-free form). Experiments were done on Varian Unityplus 500 and Unity 600 spectrometers at 23°C. Most of the NMR-observable ^1H (95.4%), ^{15}N (88.5%), and ^{13}C (88.4%) atoms were assigned by means of the following three-dimensional experiments: ^{15}N-edited total correlation spectroscopy–heteronuclear multiple quantum coherence (TOCSY-HMQC), HNHB, CBCA(CO)NH, HNCACB, H(CCO)NH, HNCO, and HCCH-TOCSY to demonstrate $C\alpha H(i)/C\beta H(i)$-$^{15}N(i)$-$NH(i)$, $C\beta H(i)$-$^{15}N(i)$-$NH(i)$, $^{13}C\beta/C\alpha(i-1)$-$^{15}N(i)$-$NH(i)$, $NH(i)$-$^{15}N(i)$-$^{13}C\beta/C\alpha(i)$, $H_\gamma(i-1)$-$^{15}N(i)$-$NH(i)$, $NH(i)$-$^{15}N(i)$-$^{13}CO(i-1)$, and $H(-^{13}C_\gamma$-$^{13}C_\lambda$-H_λ correlations, respectively (*i* refers to the residue number, whereas *j* and *k* refer to the carbon positions along a side chain). Details of these experiments and original references are provided elsewhere [J. B. Ames, T. Tanaka, L. Stryer, M. Ikura, *Biochemistry* **33**, 10743 (1994); S. Grzesiek, J. Anglister, A. Bax, *J. Magn. Reson.* **101**, 114 (1993)]. Structure calculations used 534 intraresidue, 431 sequential, 161 short-range, and 452 long-range nuclear Overhauser effect (NOE) distances, as well as 87 dihedral and 128 hydrogen bond restraints. The NOE restraints were derived from three dimensional ^{13}C- and ^{15}N-separated NOE spectra [D. R. Muhandiram, N. A. Farrow, G.-Y. Xu, S. H. Smallcombe, L. E. Kay, *J. Magn. Reson.* **102**, 317 (1993); O. Zhang, L. E. Kay, J. P. Oliver, J. D. Forman-Kay, *J. Biomol. NMR* **4**, 845 (1994)] and three-dimensional simultaneous $^{13}C/^{15}N$-separated NOE spectra [S. Pascal, D. R. Muhandiram, T. Yamazaki, J. D. Forman-Kay, L. E. Kay, *J. Magn. Reson.* **101**, 197 (1994)] with 100 ms mixing times, and from two-dimensional homonuclear NOESY spectra with 50 and 200 ms mixing times. The NOEs were classified as 0 to 2.7, 0 to 3.3, and 0 to 5.0 Å on the basis of crosspeak intensity. Val and Leu methyl groups were stereospecifically assigned from the compatibility of rotamer states with NOE intensities. Phi and psi dihedral angle restraints were obtained from coupling constants measured from $^1H/^{15}N$ HMQC-J spectra [L. E. Kay and A. Bax, *J. Magn. Reson.* **86**, 110 (1990)] and from ^{13}C chemical shift indices [D. S. Wishart and B. D. Sykes, *J. Biomol. NMR* **4**, 171 (1993)]. Hydrogen bonds were included as pairs of distance restraints in the final structure calculations based on the identification of slowly exchanging amide hydrogens from $^1H/^{15}N$ HSQC spectra obtained in ^2H_2O and by visual inspection of preliminary structures derived solely from the NOE data. Structure calculations used a simulated annealing protocol [M. Nilges, A. M. Gronenborn, A. T. Brünger, G. M. Clore, *Protein Eng.* **2**, 27 (1988)] in a strategy previously described [S. Bagby, T. S. Harvey, S. G. Eagle, S. Inouye, M. Ikura, *Structure* **2**, 107 (1994)]. Fifty independent structures of amino acids 1 to 104 (the remainder are relatively disordered because of the lack of discernible long-range NOEs and poor chemical shift dispersion) were calculated. Although Ca^{2+} was present in the protein samples, it was not included in the calculations because of the lack of unambiguous NMR constraints.
6. R. J. Poljak *et al.*, *Proc. Natl. Acad. Sci. U.S.A.* **71**, 3440 (1974).
7. Single-letter abbreviations for the amino acid residues are as follows: A, Ala; C, Cys; D, Asp; E, Glu; F, Phe; G, Gly; H, His; I, Ile; K, Lys; L, Leu; M, Met; N, Asn; P, Pro; Q, Gln; R, Arg; S, Ser; T, Thr; V, Val; W, Trp; X, any residue; and Y, Tyr.
8. O. W. Blaschuk, R. Sullivan, S. David, Y. Pouliot, *Dev. Biol.* **139**, 227 (1990).
9. P. Moingeon *et al.*, *Immunol. Rev.* **111**, 111 (1989); E. Y. Jones, *Curr. Opin. Struct. Biol.* **3**, 846 (1993).
10. A. R. Arulanandam *et al.*, *Proc. Natl. Acad. Sci. U.S.A.* **90**, 11613 (1993); C. Somoza, P. C. Driscoll, J. G. Cyster, A. F. Williams, *J. Exp. Med.* **178**, 549 (1993).
11. M. Ozawa, J. Engel, R. Kemler, *Cell* **63**, 1033 (1990).
12. M. Overduin *et al.*, data not shown.
13. A. H. Huber *et al.*, *Neuron* **12**, 717 (1994).
14. S. Pokutta, K. Herrenknecht, R. Kemler, J. Engel, *Eur. J. Biochem.* **223**, 1019 (1994).
15. M. Ozawa *et al.*, *Mech. Dev.* **33**, 49 (1990).
16. A. Nagafuchi *et al.*, *Nature* **329**, 341 (1987); M. Ozawa and R. Kemler, *J. Cell Biol.* **111**, 1645 (1990).
17. A. T. Brünger, *X-PLOR Version 3.1: A System for X-ray Crystallography and NMR* (Yale Univ. Press, New Haven, CT, 1993).

18. We thank L. E. Kay for providing pulse sequences. Supported in part by grants from the Medical Research Council of Canada (MRCC) and the Human Frontier Science Program Organization. M.O., T.S.H., and S.B. thank the National Cancer Institute of Canada, the North Atlantic Treaty Organization, and MRCC, respectively, for postdoctoral fellowships. M.I. holds an MRCC scholarship.

12 October 1994; accepted 21 December 1994

Transcription Factor ATF2 Regulation by the JNK Signal Transduction Pathway

Shashi Gupta, Debra Campbell, Benoit Dérijard, Roger J. Davis*

Treatment of cells with pro-inflammatory cytokines or ultraviolet radiation causes activation of the c-Jun NH_2-terminal protein kinase (JNK). Activating transcription factor–2 (ATF2) was found to be a target of the JNK signal transduction pathway. ATF2 was phosphorylated by JNK on two closely spaced threonine residues within the NH_2-terminal activation domain. The replacement of these phosphorylation sites with alanine inhibited the transcriptional activity of ATF2. These mutations also inhibited ATF2-stimulated gene expression mediated by the retinoblastoma (Rb) tumor suppressor and the adenovirus early region 1A (E1A) oncoprotein. Furthermore, expression of dominant-negative JNK inhibited ATF2 transcriptional activity. Together, these data demonstrate a role for the JNK signal transduction pathway in transcriptional responses mediated by ATF2.

Activating transcription factor–2 [ATF2 (also designated CRE-BP1)] is a member of a group of transcription factors that bind to a similar sequence located in the promoters of many genes (*1*). There has been considerable interest in the role of ATF2 because this transcription factor binds to several viral proteins, including the oncoprotein E1A (*2*, *3*), the hepatitis B virus X protein (*4*), and the human T cell leukemia virus–I Tax protein (*5*). ATF2 also interacts with the tumor suppressor gene product Rb (*6*), the high mobility group protein HMG I(Y) (*7*), and the transcription factors nuclear factor–κB (NF-κB) (*7*) and c-Jun (*8*). These protein-protein interactions lead to increased transcriptional activity. The function of ATF2 may therefore be determined

S. Gupta and D. Campbell, Program in Molecular Medicine, Department of Biochemistry and Molecular Biology, University of Massachusetts Medical School, Worcester, MA 01605, USA.

B. Dérijard and R. J. Davis, Program in Molecular Medicine and Howard Hughes Medical Institute, University of Massachusetts Medical School, Worcester, MA 01605, USA.

*To whom correspondence should be addressed.

by its interaction with these proteins. ATF2 may also be the direct target of a signal transduction pathway. To test this hypothesis, we investigated the potential regulation of ATF2 by phosphorylation.

We used an in-gel protein kinase assay to detect enzymes that phosphorylated ATF2 (9). This analysis demonstrated that ATF2 was a substrate for the 46-kD JNK1 (*10*) and 55-kD JNK2 (*11*) protein kinases (Fig. 1). These protein kinases are activated in cells exposed to pro-inflammatory cytokines or ultraviolet (UV) light (*10–13*) by phosphorylation on Thr and Tyr (*10*). Deletion analysis indicated that the NH_2-terminal domain of ATF2 was phosphorylated by JNK1 (Fig. 2). Progressive NH_2-terminal deletions of residues 1 to 20 or 1 to 40 caused no change in the extent of ATF2 phosphorylation. However, deletion of residues 1 to 60 blocked phosphorylation of the NH_2-terminal domain of ATF2 (Fig. 2B). These data indicate that JNK1 phosphorylates ATF2 at a site (or sites) located between residues 40 to 109 (Fig. 2B). Like the activation domain of c-Jun (*10–12, 14*), this region of ATF2 may also contain a binding site for JNK protein kinases. To test this hypothesis, we used a solid-phase kinase assay. JNK1 was incubated with immobilized ATF2, unbound JNK1 was removed by extensive washing, and bound JNK1 was detected by incubation with [γ-^{32}P]adenosine triphosphate (ATP). This assay demonstrated that JNK1 bound to and phosphorylated ATF2 (Fig. 2C). These observations were confirmed by measurement of the direct binding interaction of JNK1 with wild-type and mutated ATF2 molecules (Fig. 2D). Together, these data establish that residues 20 to 60 of ATF2 are required for binding and phosphorylation by JNK1 (Fig. 2). A similar binding interaction between ATF2 and the 55-kD JNK2 protein kinase was also observed (*15*).

Phosphorylation by JNK reduced the electrophoretic mobility of ATF2 (Fig. 3A). Phosphoamino acid analysis of the full-length ATF2 molecule (residues 1 to 505) demonstrated that JNK phosphorylated both Thr and Ser residues. The major sites of Thr and Ser phosphorylation were located in the NH_2- and COOH-terminal domains, respectively (Fig. 3B). The NH_2-terminal sites of phosphorylation were identified as Thr^{69} and Thr^{71} by phosphopeptide mapping and mutational analysis (*15*). The sites of Ser phosphorylation in the COOH-terminal domain remain to be identified. Site-directed mutagenesis demonstrated that the replacement of Thr^{69} and Thr^{71} with Ala eliminated the phosphorylation of ATF2 on Thr (Fig. 3B). These sites of Thr phosphorylation are located in a region of ATF2 that is distinct from the subdomain required for JNK binding (residues 20 to 60) (Fig. 2).

To investigate whether JNK phosphorylates ATF2 in vivo, we examined the effect of JNK activation on the properties of ATF2. JNK is activated by treatment of cells with pro-inflammatory cytokines or UV radiation (*10–13*). In initial studies, we examined the effect of UV light on the electrophoretic mobility of ATF2 during SDS–polyacrylamide gel electrophoresis (PAGE) by protein immunoblot analysis. UV radiation caused JNK activation and a reduction in the electrophoretic mobility of ATF2 (Fig. 4). This mobility shift is similar to that caused by JNK phosphorylation of ATF2 in vitro (Fig. 3). A shift in the electrophoretic mobility of ATF2 was also observed when CHO cells were incubated with the pro-inflammatory cytokine interleukin-1 (IL-1). Smaller effects on both JNK activity and ATF2 electrophoretic mobility were observed after treatment of cells with serum (Fig. 4).

The observation that JNK activation is associated with an electrophoretic mobility shift of ATF2 suggests that ATF2 may be a substrate for JNK in vivo. We therefore investigated the effect of UV radiation on the properties of wild-type (Thr^{69,71}) and phosphorylation-defective (Ala^{69,71}) ATF2 molecules. Exposure to UV caused a decrease in the electrophoretic mobility of both endogenous and overexpressed wild-type ATF2 (Fig. 5A). This change in electrophoretic mobility was associated with increased ATF2 phosphorylation (Fig. 5B).

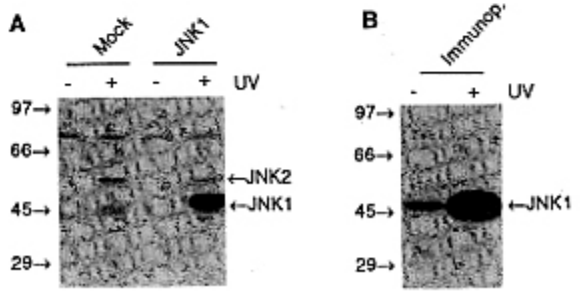

Fig. 1. ATF2 is a substrate for JNK protein kinases. COS-1 cells were transfected without and with epitope-tagged JNK1 (*26*). Some cultures were exposed to UV radiation (40 J/m^2) and incubated for 1 hour at 37°C. The protein kinase activity in the cell lysates (**A**) and JNK1 immunoprecipitates (**B**) was examined with an in-gel assay, and the substrate (GST-ATF2, residues 1 to 505) polymerized in the gel (*9*). The cell lysates demonstrate the presence of 46-kD and 55-kD protein kinases that phosphorylate ATF2 in extracts prepared from UV-irradiated cells. The 46-kD and 55-kD protein kinases were identified as JNK1 (*10*) and JNK2 (*11*), respectively.

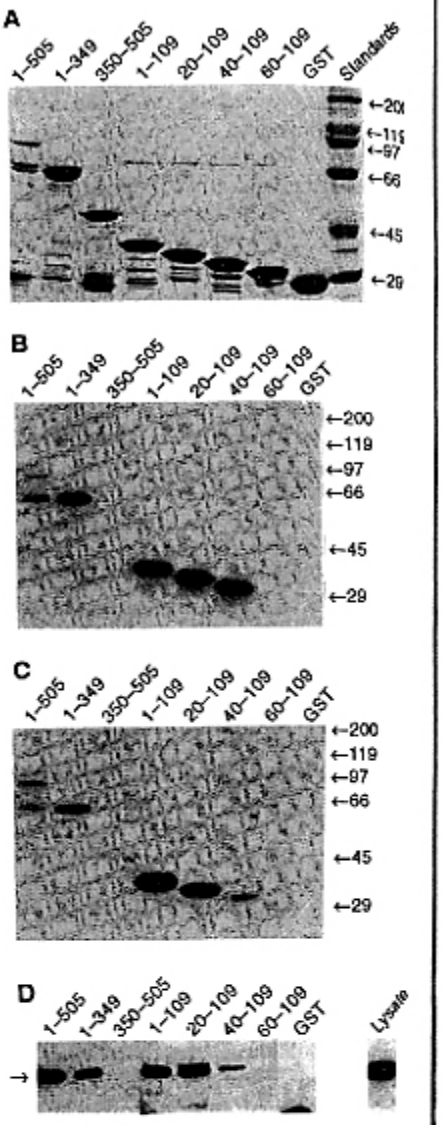

Fig. 2. Binding of JNK to ATF2 and phosphorylation of the NH_2-terminal activation domain. (**A**) Purified GST-ATF2 fusion proteins (*25*) were resolved by SDS-PAGE and stained with Coomassie blue. Each lane on the gel is labeled with the residues of ATF2 that are fused to GST. Molecular size standards (kilodaltons) are indicated on the right. (**B**) The phosphorylation of GST-ATF2 fusion proteins by JNK1 isolated from UV-irradiated cells was examined in an immunocomplex kinase assay (*9*). (**C**) The phosphorylation of immobilized GST-ATF2 fusion proteins was examined in a solid-phase kinase assay (*9*). JNK1 from UV-irradiated cells was incubated with GST-ATF2 fusion proteins bound to glutathione-agarose. The agarose beads were washed extensively to remove the unbound JNK1. Phosphorylation of the GST-ATF2 fusion proteins by the bound JNK1 protein kinase was examined by addition of [γ-^{32}P]ATP. (**D**) The binding of JNK1 to ATF2 was examined by incubation of GST-fusion proteins bound to glutathione-agarose beads with cell lysate (*27*). The agarose beads were incubated for 1 hour at 4°C and then washed extensively. JNK1 present in the cell lysate and bound to the beads was detected by protein immunoblot analysis (arrow).

Both the electrophoretic mobility shift and the increased phosphorylation were blocked by the replacement of Thr^{69} and Thr^{71} with Ala (Fig. 5B). This mutation also blocked the phosphorylation of ATF2 on Thr residues in vivo (Fig. 5C). Furthermore, mutation of ATF2 at Thr^{69} and Thr^{71} resulted in the loss of two tryptic phosphopeptides in maps of ATF2 isolated from UV-irradiated cells (Fig. 5D). These phosphopeptides correspond to mono- and bis-phosphorylated peptides containing Thr^{69} and Thr^{71}. Both of these phosphopeptides were found in maps of ATF2 phosphorylated by JNK1 in vitro (Fig. 5D). However, the amount of bis-phosphorylation on Thr^{69} and Thr^{71} was greater in vivo than in vitro. Taken together, these data indicate that ATF2 is a substrate for JNK protein kinases in vivo.

The identification of ATF2 as a JNK substrate in vivo suggests that ATF2 activity may be regulated by the JNK protein kinase signal transduction pathway. The DNA binding activity of bacterially expressed ATF2 is increased by phosphorylation in vitro (*16*). We therefore investigated the effect of JNK activation on the DNA binding properties of ATF2 (*17*). Irradiation of cells with UV light caused no change in the DNA binding activity of ATF2 measured in nuclear extracts (*15*). Thus, JNK activation does not appear to regulate ATF2 DNA binding activity in vivo.

The location of the phosphorylation sites Thr^{69} and Thr^{71} within the NH_2-terminal activation domain of ATF2 suggests that these sites may regulate transcriptional activity. We therefore examined the effect of point mutations at Thr^{69} and Thr^{71} on ATF2-stimulated expression of a luciferase reporter gene. Similar amounts of the wild-type and mutated ATF2 molecules were detected by immunoblot analysis (*15*). Replacement of Thr^{69} or Thr^{71} with Ala caused a decrease in luciferase expression mediated by ATF2 (Fig. 6A). Replacement of Thr^{69} with Glu also decreased reporter gene expression, which indicates that the acidic Glu residue does not functionally substitute for phosphorylated Thr. Similar transcriptional activities were detected for mutant ATF2 proteins containing single mutations at Thr^{69} and Thr^{71} or mutations at both residues (Fig. 6A). This observation suggests that both phosphorylation sites are required for the transcriptional activity of ATF2. Consistent with this conclusion is the finding that ATF2 is phosphorylated on both Thr^{69} and Thr^{71} in vivo (Fig. 5). The effect of phosphorylation to increase transcriptional activity may be mediated by phosphorylation-dependent binding of ATF2 to a co-activator such as the CREB binding protein CBP (*18*).

The effect of point mutations at Thr^{69} and Thr^{71} on the transcriptional activity of ATF2 (Fig. 6A) indicates that the phosphorylation of ATF2 by JNK may be physiologically significant. To test this hypothesis, we investigated the effect of a dominant-interfering JNK1 mutant on ATF2 function. The binding of JNK1 to the NH_2-terminal activation domain of ATF2 (Fig. 2) suggests that a catalytically inactive JNK1 protein kinase may function as a dominant inhibitor. JNK1 protein kinase activation requires phosphorylation on Thr^{183} and Tyr^{185} (*10*). We therefore con-

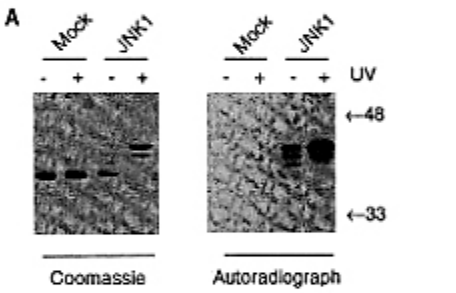

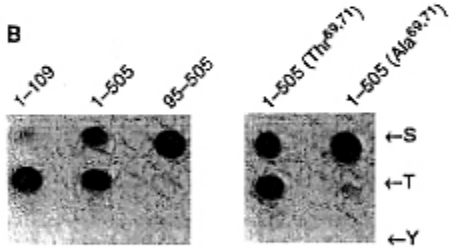

Fig. 3. Phosphorylation of the NH_2-terminal activation domain of ATF2 on Thr^{69} and Thr^{71} by JNK1. (**A**) Mock-transfected and JNK1-transfected COS cells (*26*) were treated without and with UV (40 J/m^2) radiation. The epitope-tagged JNK1 was isolated by immunoprecipitation with the M2 monoclonal antibody. The phosphorylation of GST-ATF2 (residues 1 to 109) was examined in an immunocomplex kinase assay (*9*). The GST-ATF2 was resolved from other proteins by SDS-PAGE and stained with Coomassie blue. The phosphorylation of GST-ATF2 was detected by autoradiography. (**B**) GST fusion proteins containing full-length ATF2 (residues 1 to 505), an NH_2-terminal fragment (residues 1 to 109), and a COOH-terminal fragment (residues 95 to 505) were phosphorylated with JNK1 and analyzed by phosphoamino acid analysis (*9*). S, phosphoserine; T, phosphothreonine; Y, phosphotyrosine.

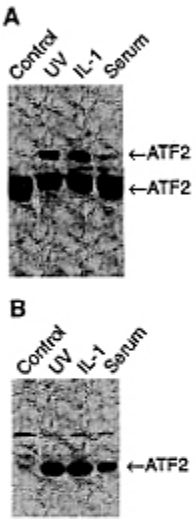

Fig. 4. Reduced electrophoretic mobility of JNK-activated ATF2. (**A**) CHO cells were treated with UV-C (40 J/m^2), IL-1α (10 ng/ml), or serum (20%). The cells were incubated for 30 min at 37°C before harvesting. The electrophoretic mobility of ATF2 after SDS-PAGE was examined by protein immunoblot analysis (*28*). (**B**) JNK protein kinase activity present in the cell extracts was measured by immunocomplex kinase assay (*9*). JNK was immunoprecipitated with a polyclonal antibody, and the phosphorylation of the substrate GST-ATF2 (residues 1 to 109) was examined after addition of [γ-^{32}P]ATP. The phosphorylated GST-ATF2 was detected after SDS-PAGE by autoradiography.

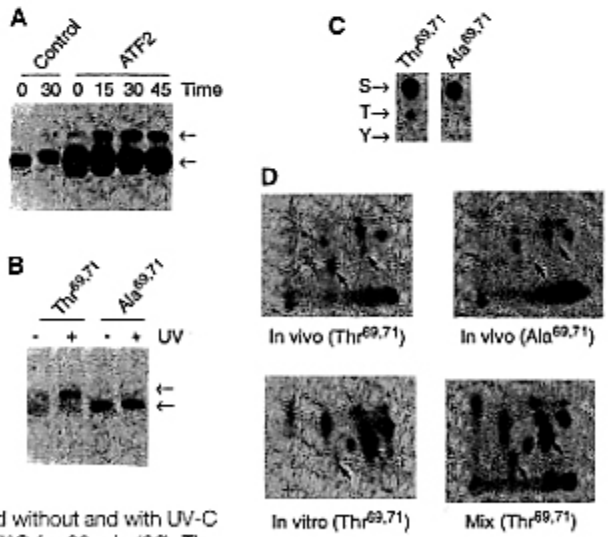

Fig. 5. Increased ATF2 phosphorylation after activation of JNK in vivo. (**A**) COS-1 cells were transfected without (control) and with an ATF2 expression vector (*26*). The effect of exposure of the cells to UV-C (40 J/m^2) was examined. After irradiation, the cells were incubated for defined times at 37°C and then collected. The electrophoretic mobility of ATF2 during SDS-PAGE was examined by protein immunoblot analysis (*28*). The two electrophoretic mobility forms of ATF2 are indicated with arrows. (**B**) The phosphorylation state of wild-type ($Thr^{69,71}$) ATF2 and mutated ($Ala^{69,71}$) ATF2 was examined in cells labeled with ^{32}P, treated without and with UV-C (40 J/m^2), and then incubated at 37°C for 30 min (*26*). The ATF2 proteins were isolated by immunoprecipitation and analyzed by SDS-PAGE and autoradiography (*9*). (**C**) The phosphorylated ATF2 proteins isolated from UV-irradiated cells were examined by phosphoamino acid analysis (*9*). (**D**) Tryptic phosphopeptide mapping was used to compare ATF2 phosphorylated in vitro by JNK1 with ATF2 phosphorylated in vivo. A map was also prepared with a sample composed of equal amounts of in vivo– and in vitro–phosphorylated ATF2 (Mix). The origin of the maps is indicated with a cross. Two phosphopeptides are indicated with arrows.

structed a catalytically inactive JNK1 mutant by replacing the sites of activating Thr and Tyr phosphorylation with Ala and Phe, respectively. Expression of wild-type JNK1 caused a small increase in serum-stimulated ATF2 transcriptional activity (Fig. 6B). In contrast, dominant-negative JNK1 inhibited both control and serum-stimulated ATF2 activity. This inhibitory effect may result from the nonproductive binding of the JNK1 mutant to the ATF2 activation domain. These data provide evidence that JNK1 is a physiologically relevant protein kinase that interacts with ATF2 in vivo.

The tumor suppressor gene product Rb binds to ATF2 and increases ATF2-stimulated gene expression (*6*). Similarly, the adenovirus oncoprotein E1A associates with the DNA binding domain of ATF2 (*2*) and increases ATF2-stimulated gene expression by a mechanism that requires the NH_2-terminal activation domain of ATF2 (*2*, *3*, *19*). Rb and E1A increased ATF2-stimulated gene expression in experiments with both wild-type ($Thr^{69,71}$) and mutated ($Ala^{69,71}$) ATF2 molecules (Fig. 6, C and D). However, the phosphorylation-defective ATF2 caused a lower level of reporter gene expression than did wild-type ATF2 (Fig. 6, C and D). Together, these data indicate a requirement for ATF2 phosphorylation (on Thr^{69} and Thr^{71}) together with Rb or E1A for maximal transcriptional activity. Thus, Rb and E1A act in concert with ATF2 phosphorylation to control transcriptional activity.

Ultraviolet irradiation and pro-inflammatory cytokines (tumor necrosis factor and IL-1) are potent activators of the JNK protein kinase (*10*–*13*). We have demonstrated that the transcription factor ATF2 is a target of the JNK signal transduction pathway. JNK phosphorylates ATF2 (Fig. 1) and related members of the ATF2 group of transcription factors [ATFa (*15*) and CRE-BPa]. ATF2 binds to CRE-like elements [T(G/T)ACGTCA] in the promoters of many genes. Indeed, a specific role for ATF2 in the expression of human T cell leukemia virus–1 (*5*), transforming growth factor–β2 (*6*), interferon β (*7*), and E-selectin (*20*) has been established. In addition, ATF2 is implicated in the function of a T cell–specific enhancer (*21*). Thus, the activation of ATF2 can account for the induction of gene expression by means of CRE-like elements by the JNK signal transduction pathway. ATF2 also binds to CRE-like elements as a heterodimer with partners such as c-Jun (*8*). Both ATF2 and c-Jun are phosphorylated by JNK (*22*). The ATF2–c-Jun heterodimer may therefore be a physiologically relevant target of the JNK signal transduction pathway. Indeed, a role for activated ATF2–c-Jun heterodimers is implicated in oncogenic transformation (*23*).

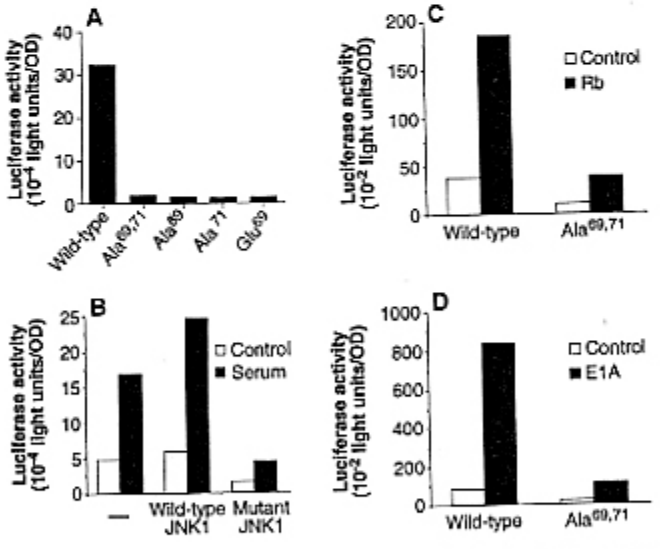

Fig. 6. Inhibition of ATF2-stimulated gene expression by mutation of the phosphorylation sites Thr^{69} and Thr^{71}. A fusion protein consisting of ATF2 and the GAL4 DNA binding domain was expressed in CHO cells (*29*). ATF2 transcriptional activity was examined with a luciferase reporter plasmid. Transfection efficiency was examined by cotransfection of a control plasmid that expresses β-galactosidase activity. The data are reported as the mean activity ratio of luciferase–β-galactosidase determined in three experiments. The SD was less than 10% of the mean for each data point. Control experiments with the GAL4 DNA binding domain without ATF2 sequences caused a low level of luciferase activity [<50 light units/optical density (OD)]. (**A**) The effect of point mutations at the ATF2 phosphorylation sites Thr^{69} and Thr^{71} was examined by expression of GAL4-ATF2 (residues 1 to 109) in serum-treated CHO cells. (**B**) ATF2 transcriptional activity in CHO cells was examined with GAL4-ATF2 (residues 1 to 109) and a luciferase reporter plasmid (*29*). The effect of expression of wild-type JNK1 (Thr^{183} and Tyr^{185}) and dominant-negative JNK1 (Ala^{183} and Phe^{185}) was examined. Control experiments were done with mock-transfected cells (−). The CHO cells were serum-starved for 18 hours and then incubated without or with serum for 4 hours. (**C**) ATF2 transcriptional activity was investigated with a luciferase reporter plasmid and GAL4-ATF2 (residues 1 to 505) (*29*). Expression of Rb was also examined. No effect of Rb on luciferase activity was detected in the absence of GAL4-ATF2 (*15*). (**D**) ATF2 transcriptional activity was investigated with a luciferase reporter plasmid and GAL4-ATF2 (residues 1 to 505) (*29*). The effect of expression of the adenovirus oncoprotein E1A was examined. No effect of E1A on luciferase activity was detected in the absence of GAL4-ATF2 (*15*).

REFERENCES AND NOTES

1. E. B. Ziff, *Trends Genet.* **6**, 69 (1990).
2. F. Liu and M. R. Green, *Nature* **368**, 520 (1994); *Cell* **61**, 1217 (1990).
3. H. A. M. Abdel-Hafiz, C.-Y. Chen, T. Marcell, D. J. Kroll, J. P. Hoeffler, *Oncogene* **8**, 1161 (1993); K. J. Flint and N. C. Jones, *ibid.* **6**, 2019 (1991).
4. H. F. Maguire, J. P. Hoeffler, A. Siddiqui, *Science* **252**, 842 (1991).
5. S. Wagner and M. R. Green, *ibid.* **262**, 395 (1993); A. A. Franklin *et al.*, *J. Biol. Chem.* **268**, 21225 (1993).
6. S.-J. Kim *et al.*, *Nature* **358**, 331 (1992).
7. W. Du, D. Thanos, T. Maniatis, *Cell* **74**, 887 (1993).
8. D. M. Benbrook and N. C. Jones, *Oncogene* **5**, 295 (1990); P. F. Macgregor, C. Abate, T. Curran, *ibid.*, p. 451; L. B. Ivashkiv *et al.*, *Mol. Cell. Biol.* **10**, 1609 (1990); T. Hai and T. Curran, *Proc. Natl. Acad. Sci. U.S.A.* **88**, 3720 (1991).
9. In-gel protein kinase assays were done after SDS-PAGE by renaturation of protein kinases and incubation with [γ-^{32}P]ATP (*10*). Solid-phase protein kinase assays with immobilized glutathione-S-transferase (GST) fusion proteins were done as described (*12*). Immunocomplex kinase assays were done with Flag epitope–tagged JNK1 and the monoclonal antibody M2 (IBI-Kodak) as described (*10*). Immunocomplex protein kinase assays were also done with a rabbit antiserum prepared with recombinant JNK1 as an antigen. The cells were solubilized with buffer A [20 mM tris (pH 7.5), 10% glycerol, 1% Triton X-100, 0.137 M NaCl, 25 mM β-glycerophosphate, 2 mM EDTA, 1 mM orthovanadate, 2 mM pyrophosphate, leupeptin (10 μg/ml), and 1 mM phenylmethylsulfonyl fluoride]. JNK1 was immunoprecipitated with protein G–Sepharose bound to a rabbit polyclonal antibody to JNK or the M2 monoclonal antibody to the Flag epitope. The beads were washed three times with lysis buffer and once with kinase buffer [20 mM Hepes (pH 7.6), 20 mM $MgCl_2$, 25 mM β-glycerophosphate, 100 μM sodium orthovanadate, and 2 mM dithiothreitol]. The kinase assays were done at 25°C for 10 min with 1 μg of substrate, 20 μM adenosine triphosphate, and 10 μCi of [γ-^{32}P]ATP in 30 μl of kinase buffer. The reactions were terminated with Laemmli sample buffer, and the products were resolved by SDS-PAGE (10% gel). The incorporation of [^{32}P]phosphate was visualized by autoradiography and quantitated with a phosphorimager and ImageQuant software (Molecular Dynamics, Sunnyvale, CA). Control experiments demonstrated that the immunocomplex kinase assays were linear with enzyme concentration and time (up to 30 min). The methods used for phosphopeptide mapping and phosphoamino acid analysis were as described [E. Alvarez *et al.*, *J. Biol. Chem.* **266**, 15277 (1991)]. The horizontal dimension of the peptide maps was electrophoresis and the vertical dimension was chromatography.
10. B. Dérijard *et al.*, *Cell* **76**, 1025 (1994).
11. H. K. Sluss, T. Barrett, B. Dérijard, R. J. Davis, *Mol. Cell. Biol.* **14**, 8376 (1994); T. Kallunki *et al.*, *Genes Dev.*, in press.
12. M. Hibi, A. Lin, T. Smeal, A. Minden, M. Karin, *Genes Dev.* **7**, 2135 (1993).
13. J. M. Kyriakis *et al.*, *Nature* **369**, 156 (1994).
14. V. Adler, C. C. Franklin, A. S. Kraft, *Proc. Natl. Acad. Sci. U.S.A.* **89**, 5341 (1992).
15. S. Gupta, unpublished results.
16. H. A. M. Abdel-Hafiz *et al.*, *Mol. Endocrinol.* **6**, 2079 (1992).
17. The DNA binding activity of ATF2 was examined by electrophoretic mobility shift assay with nuclear extracts prepared from COS-1 cells [K. A. Lee and M. R. Green, *Methods Enzymol.* **181**, 20 (1990)] and a ^{32}P-labeled probe containing the sequence element GAAGTGACGTCAGTGG (*24*). Phosphatase inhibitors (25 mM β-glycerophosphate and 1 mM orthovanadate) were included in all solutions. The binding assays were done with 5 μg of nuclear extract in a final volume of 20 μl (*24*). After 15 min of

incubation at 25°C, the protein-DNA complexes were analyzed by PAGE (5% gel) in 0.5× tris-borate EDTA. The gel was dried, and the protein complexes were detected by autoradiography and quantitated by phosphorimager analysis. The ATF2-DNA complexes were identified in transient transfection assays by overexpression of ATF2. The presence of ATF2 was confirmed by supershift analysis with the monoclonal antibody F2BR-1 to ATF2 (Santa Cruz Biotechnology).

18. J. C. Chrivia *et al.*, *Nature* **365**, 855 (1993); R. P. S. Kwok *et al.*, *ibid.* **370**, 223 (1994); J. Arias *et al.*, *ibid.*, p. 226.
19. J. P. Hoeffler, *J. Invest. Dermatol.* **98**, 21S (1992); B. Chatton *et al.*, *Mol. Cell. Biol.* **13**, 561 (1993).
20. L. G. DeLuca, D. R. Johnson, M. Z. Whitley, T. Collins, J. S. Pober, *J. Biol. Chem.* **269**, 19193 (1994).
21. K. Georgopoulos, B. A. Morgan, B. A. Moore, *Mol. Cell. Biol.* **12**, 747 (1992).
22. A direct comparison of ATF2 and c-Jun as substrates for JNK in vitro demonstrates that the rate of phosphorylation of both transcription factors is similar. Therefore, JNK does not selectively phosphorylate either ATF2 or c-Jun.
23. B. M. Hagmeyer *et al.*, *EMBO J.* **12**, 3559 (1993); H. van Dam *et al.*, *ibid.*, p. 479.
24. T. Hai, F. Liu, W. J. Coukos, M. R. Green, *Genes Dev.* **3**, 2083 (1989).
25. Plasmid expression vectors encoding the JNK1 complementary DNA (cDNA) (*10*), ATF2 [pECE-ATF2 (*2*)], Rb [phuRb; P. D. Robbins, J. M. Horowitz, R. C. Mulligan, *Nature* **346**, 668 (1990)], and E1A [pSVE1a; D. H. Smith, D. M. Kegler, E. B. Ziff, *Mol. Cell. Biol.* **5**, 2684 (1985)] have been described. Bacterial expression vectors for GST-ATF2 fusion proteins were constructed by subcloning ATF2 cDNA fragments from a polymerase chain reaction (PCR) into pGEX-3X (Pharmacia-LKB Biotechnology). Point mutations were generated with mutagenic primers and overlapping PCR [S. N. Ho, H. D. Hunt, R. M Horton, J. K. Pullen, L. R. Pease, *Gene* **77**, 51 (1989)]. The sequence of all constructed plasmids was confirmed by automated sequencing with an Applied Biosystems model 373A machine. The GST-ATF2 proteins were purified as described [S. B. Smith and K. S. Johnson, *Gene* **67**, 31 (1988)].
26. CHO cells were maintained in Ham's F12 medium supplemented with 5% bovine serum albumin (Gibco-BRL). COS-1 cells were maintained in Dulbecco's modified Eagle's medium supplemented with fetal bovine serum (5%) (Gibco-BRL). Metabolic labeling with ^{32}P was performed by incubation of cells for 3 hours in phosphate-free modified Eagle's medium (Flow Laboratories, McLean, VA) supplemented with [^{32}P]orthophosphate (2 mCi/ml) (Dupont-NEN). Plasmid DNA (*25*) was transfected into CHO and COS-1 cells by the lipofectamine method (Gibco-BRL) and harvested after 48 hours of incubation. The cells were treated with IL-1α (Genzyme), exposed to UV-C radiation (*10*), or incubated with 20% fetal bovine serum (Gibco-BRL).
27. Recombinant GST-ATF2 fusion proteins (5 μg) bound to glutathione-agarose beads were incubated with cell lysates (80 μg) in 500 μl of buffer A (*9*). After 1 hour of incubation at 4°C, the beads were washed five times with binding buffer. JNK1 in the cell lysate and bound to the beads was detected by protein immunoblot analysis.
28. Cells were lysed in 20 mM tris (pH 7.5), 25 mM β-glycerophosphate, 10% glycerol, 1% Triton X-100, 0.5% (w/v) deoxycholate, 0.1% (w/v) SDS, 0.137 M NaCl, 2 mM pyrophosphate, 1 mM orthovanadate, 2 mM EDTA, leupeptin (10 μg/ml), and 1 mM phenylmethylsulfonyl fluoride. Soluble extracts were prepared by centrifugation in a microfuge for 20 min at 4°C. The extracts were incubated with 1 μg of monoclonal antibody to ATF2 (clone F2BR-1; Santa Cruz) bound to protein G–Sepharose (Pharmacia-LKB Biotechnology). After 1 hour of incubation at 4°C, the immunoprecipitates were washed three times with lysis buffer, resolved by SDS-PAGE, and electroblotted onto Immobilon P membranes (Millipore). The membranes were probed with an antibody to ATF2 (*6*), and immunocomplexes were visualized by enhanced chemiluminescence detection (Amersham International PLC).
29. The function of the ATF2 transactivation domain was examined in experiments with a fusion protein consisting of residues 1 to 505 or 1 to 109 of ATF2 and the DNA binding domain of the yeast transcription factor GAL4 as described (*2*). The activity of the GAL4-ATF2 fusion protein was measured in cotransfection assays (*26*) with the reporter plasmid pG5E1bLuc [A. Seth, F. A. Gonzalez, S. Gupta, D. L. Raden, R. J. Davis, *J. Biol. Chem.* **267**, 24796 (1992)]. This reporter plasmid contains five GAL4 sites cloned upstream of a minimal promoter element and the firefly luciferase gene. Transfection efficiency was monitored with a control plasmid that expresses β-galactosidase (pCH110; Pharmacia-LKB Biotechnology). The luciferase and β-galactosidase activity detected in cell extracts was measured [S. Gupta, A. Seth, R. J. Davis, *Proc. Natl. Acad. Sci. U.S.A.* **90**, 3216 (1993)].
30. We thank M. Dickens for preparing JNK antiserum; P. Robbins and M. R. Green for providing reagents; R. Singh for critical comments; T. Barrett and I.-H. Wu for technical assistance; and M. Shepard for secretarial assistance. Supported in part by a grant from the National Cancer Institute. R.J.D. is an investigator of the Howard Hughes Medical Institute.

5 August 1994; accepted 31 October 1994